Electronic Supplementary Information (ESI)

Boosting bifunctional electrocatalytic activity in S and N co-doped carbon nanosheets for high-efficiency Zn-air batteries

Yibo Guo[1], Sai Yao[1], Longxue Gao, An Chen, Menggai Jiao, Huijuan Cui, Zhen Zhou**

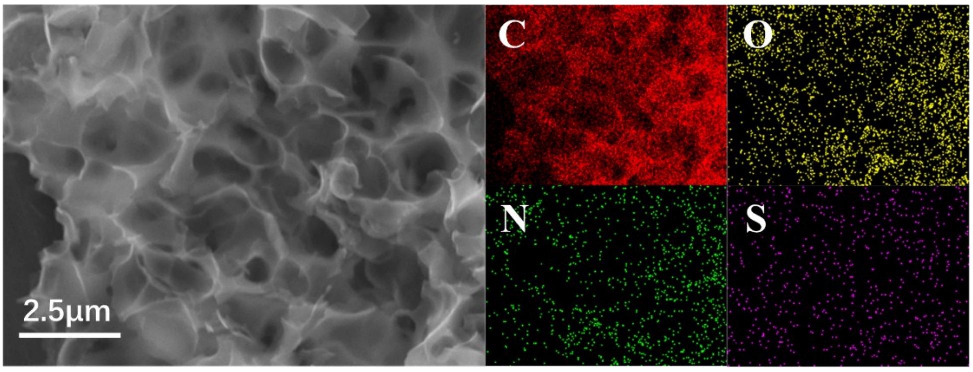

Fig.S1. SEM images and energy dispersive X-ray spectroscopy (EDS) elemental mapping of C, O, N and S of SNC.

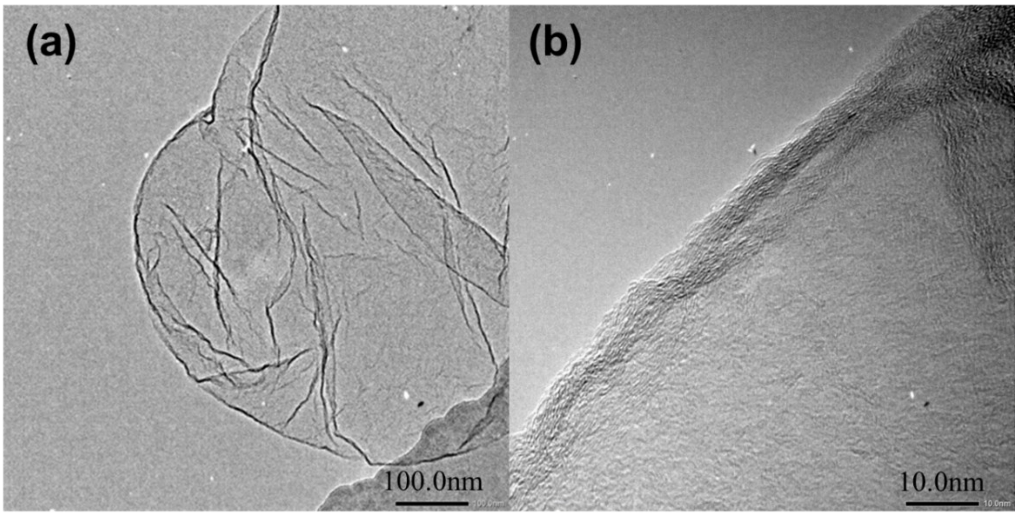

Fig. S2. (a) TEM images and (b) HRTEM image of SNC.

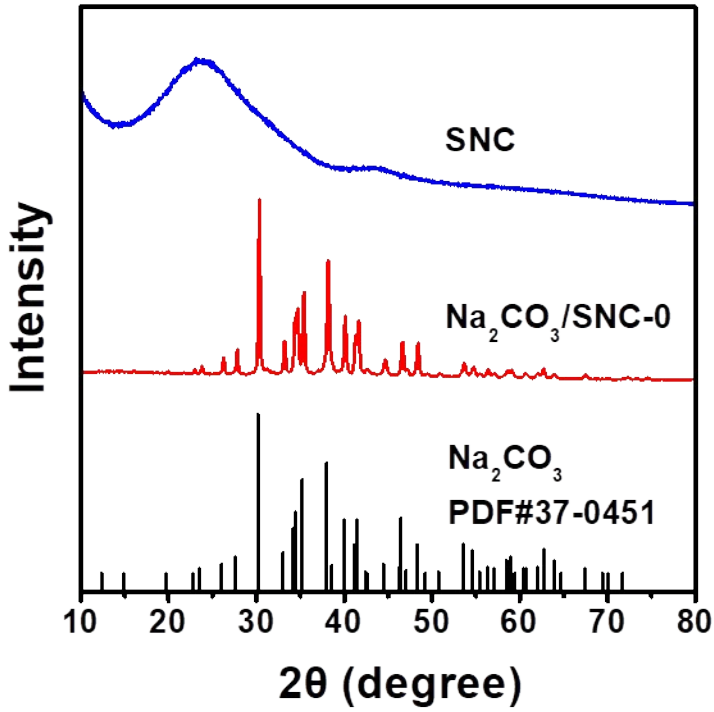

Fig. S3. XRD patterns of SNC (blue line) and the sample after fast pyrolysis (red line). Compared with the standard cards of XRD, the sample after fast pyrolysis was Na_2CO_3/SNC-0. After washing with water, the Na_2CO_3 particles were removed, leaving the carbon product which was defined as SNC-0.

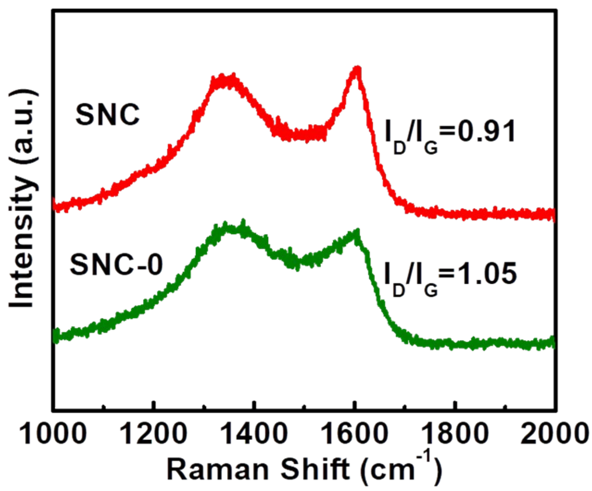

Fig. S4. Raman Spectra of SNC and SNC-0 (sample without second pyrolysis).

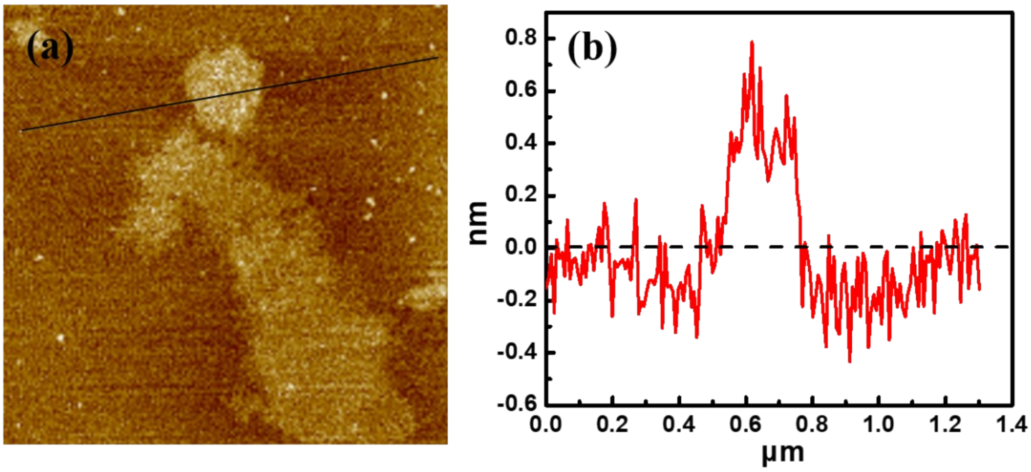

Fig. S5. AFM image of SNC. The thickness of the SNC sheet is about 1.0 nm.

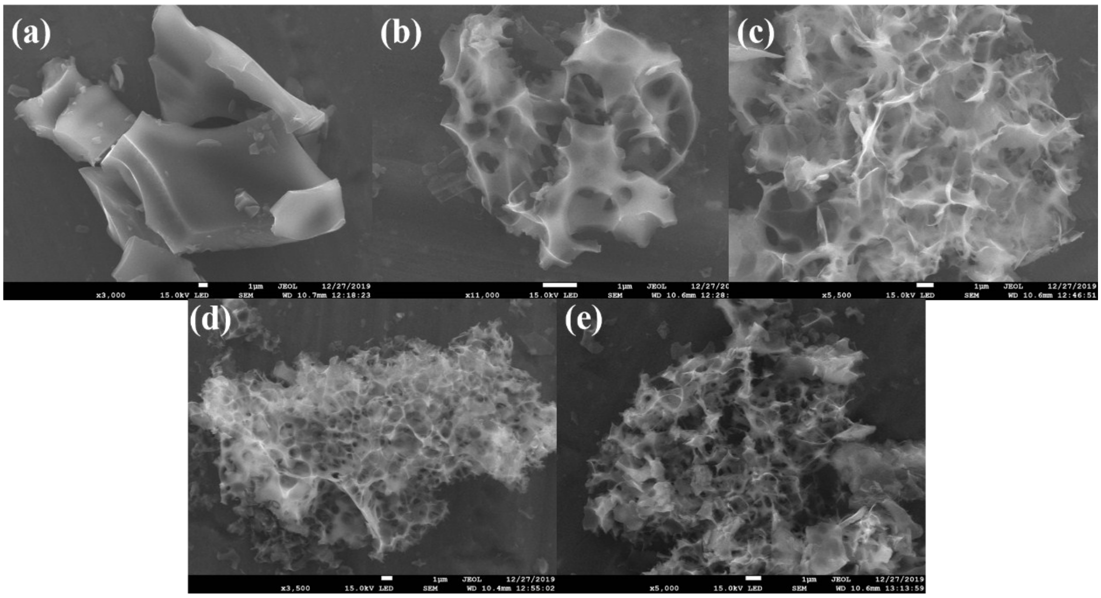

Fig. S6. SEM images of samples synthetized with different proportions of L-cysteine and Na_2CO_3. a), 1:0; b) 1:0.5; c) 1:3; d) 1:5; e) 1:7.

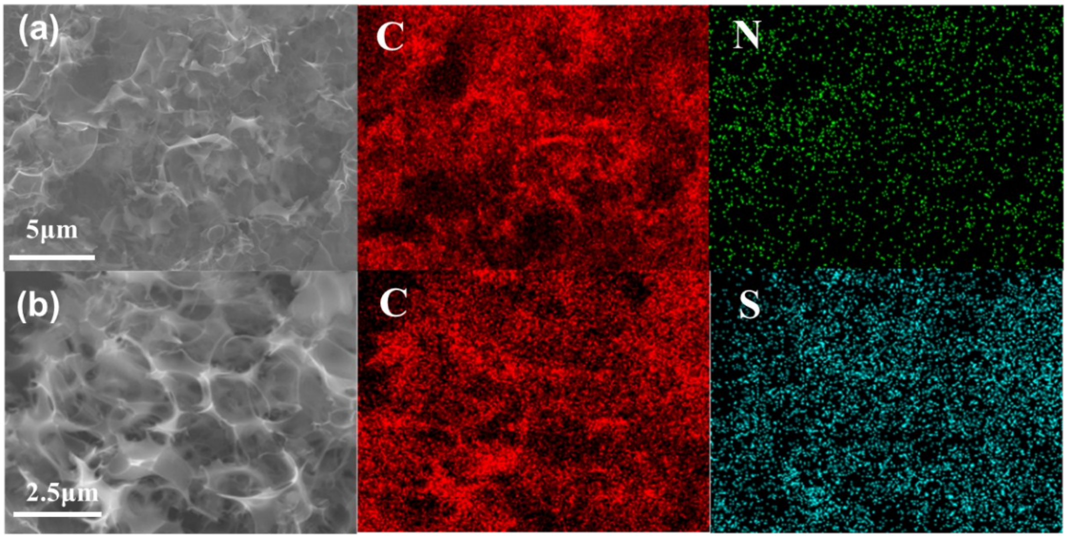

Fig. S7. (a) SEM image of NC and EDS elemental mapping images of C and N of NC. (b) SEM image of SC and EDS elemental mapping images of C, and S of SC.

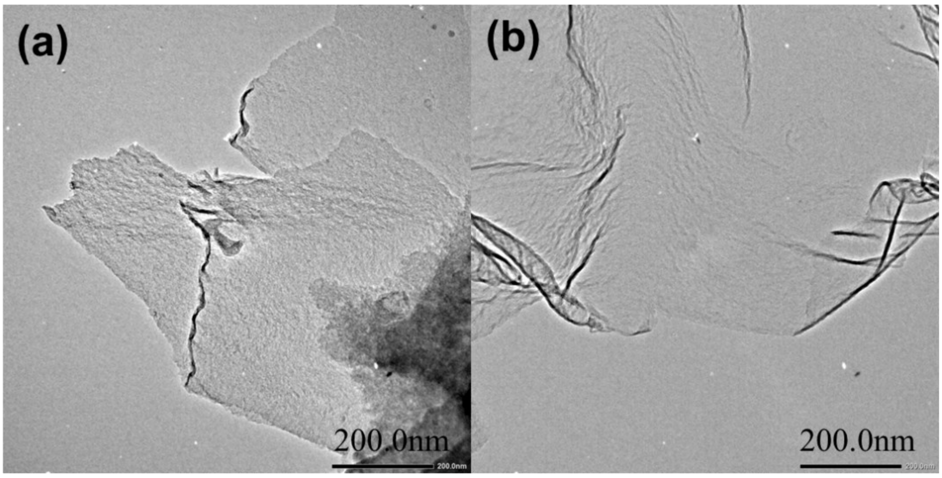

Fig. S8. (a) TEM images of NC. (b) TEM images of SC.

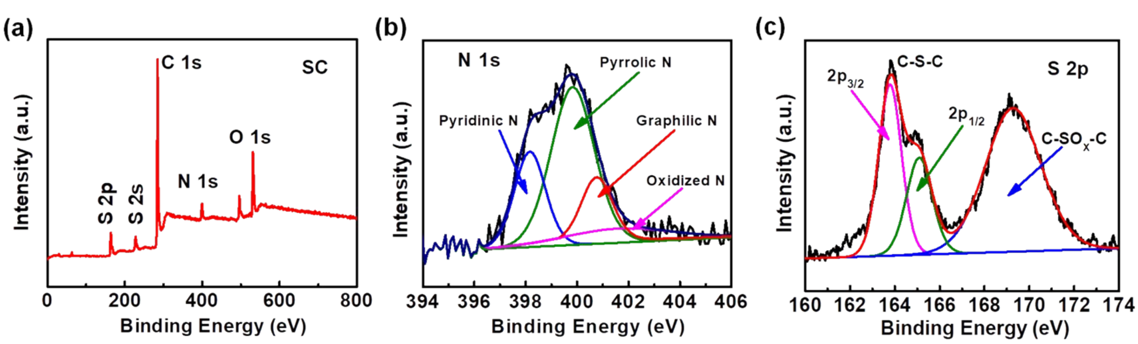

Fig. S9. (a) XPS, (b) N1s fitting results and (c) S2p fitting results of SNC-0 (sample without second pyrolysis).

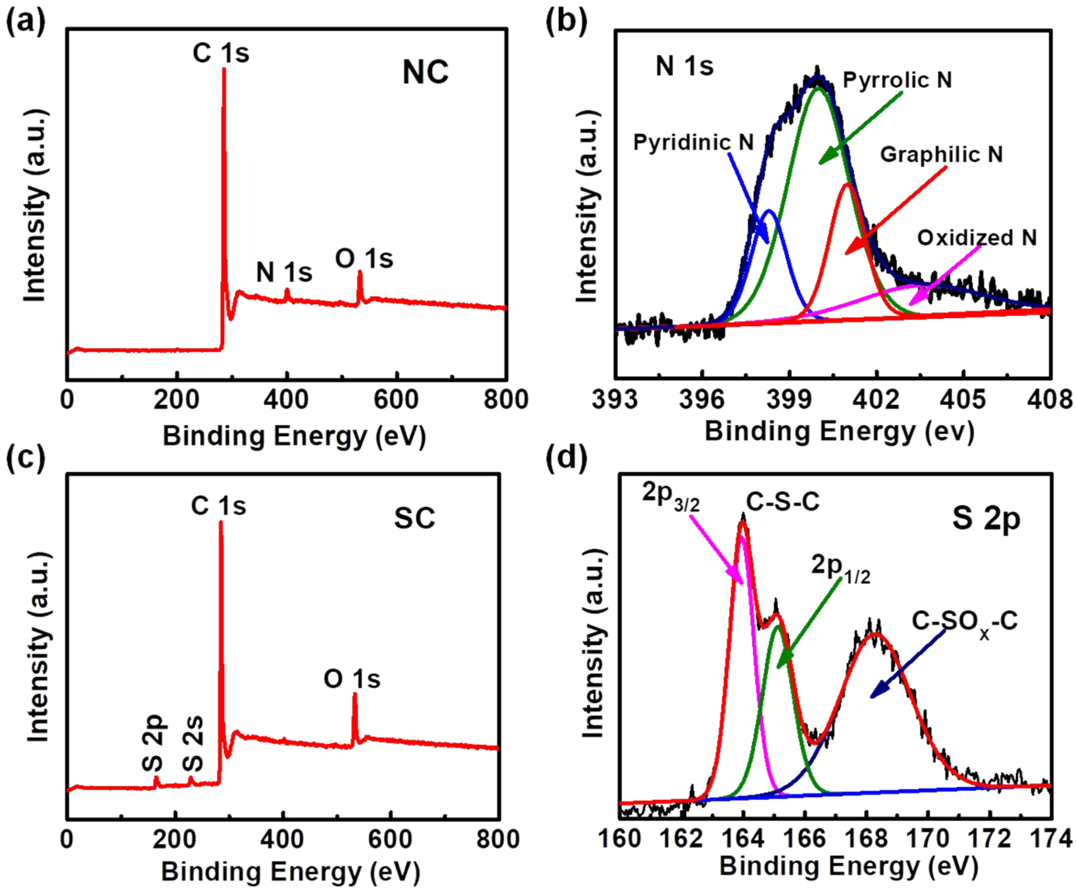

Fig. S10. (a) XPS and (b) N1s fitting results of NC; (c) XPS and (d) S2p fitting results of SC.

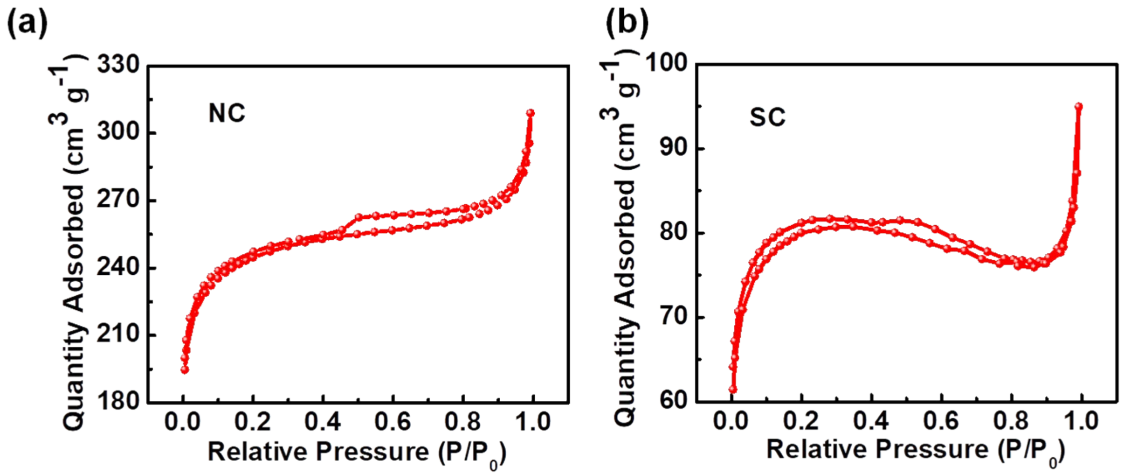

Fig. S11. N_2 adsorption-desorption isotherm curves of NC (a) and SC (b).

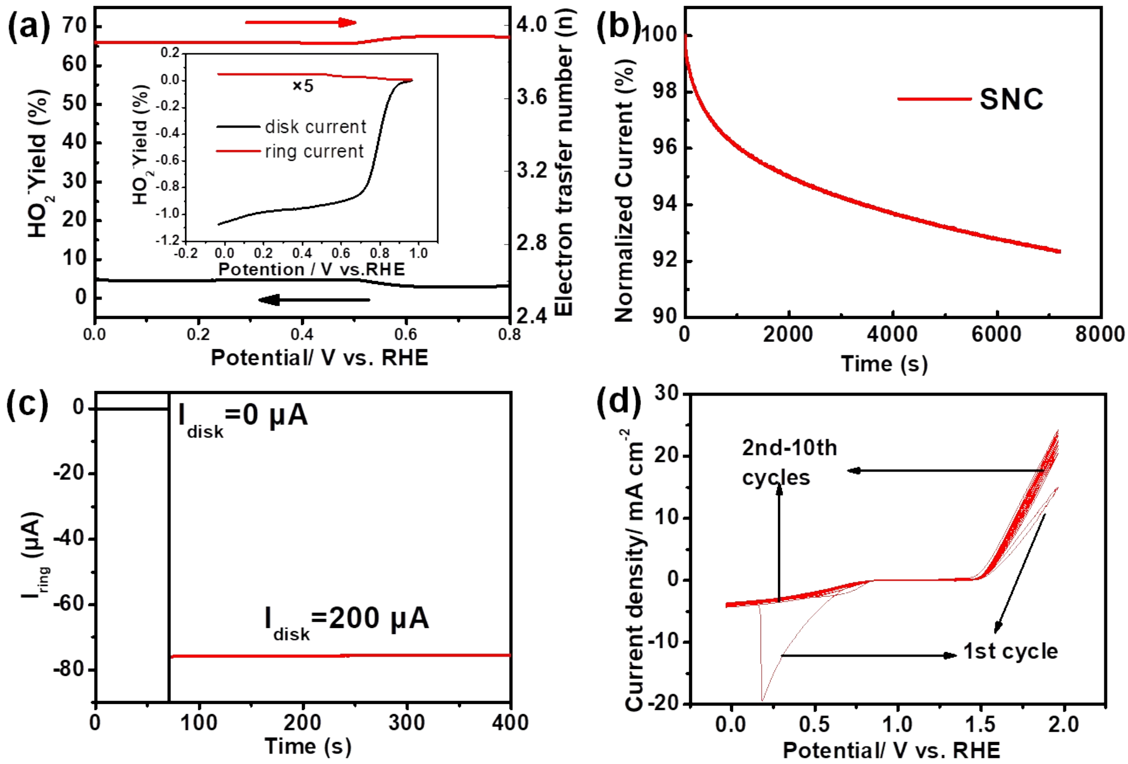

Fig. S12. (a) Electron transfer number (n) and HO_2^- yield derived from the RRDE tests for ORR, and the inset exhibits RRDE voltammograms of the SNC catalyst at 1600 rpm. The ring current is amplified by 5 for better resolution. (b) Current-time chronoamperometric response for the ORR at the half-wave potential of the SNC catalyst. (c) Ring current of SNC for OER on a RRDE at 1600 rpm with a ring potential of 0.45 V in 0.1 M KOH solution. (d) Continuous voltammetry of SNC scanning from OER to ORR with a scan rate of 5 mV s^{-1}.

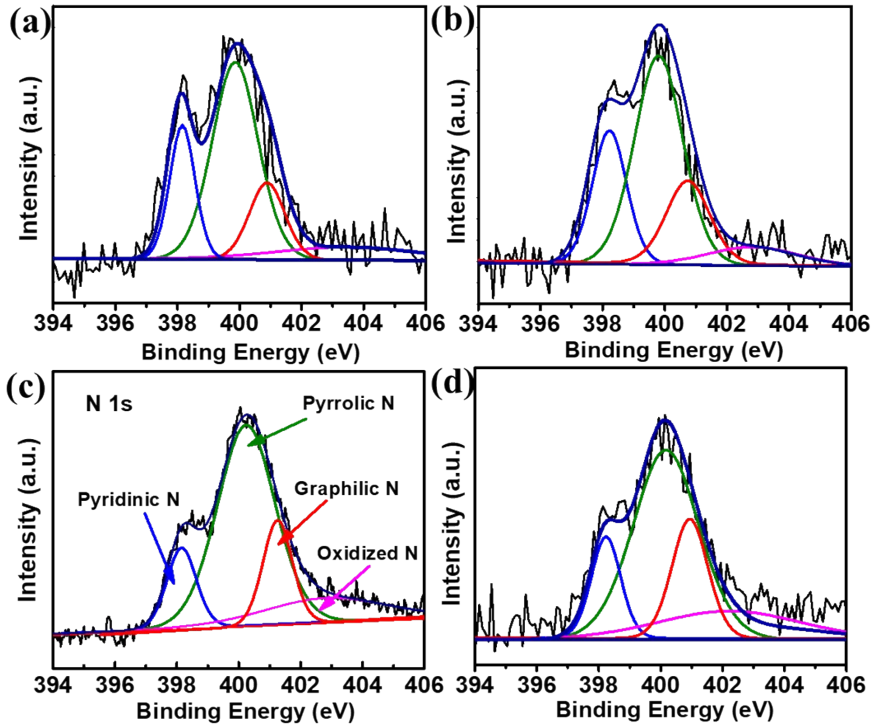

Fig. S13. N1s fitting results of SNC synthetized with different fast pyrolysis temperatures. (a) 800 ℃ (b) 900 ℃ (c) 1000 ℃ (d) 1100 ℃.

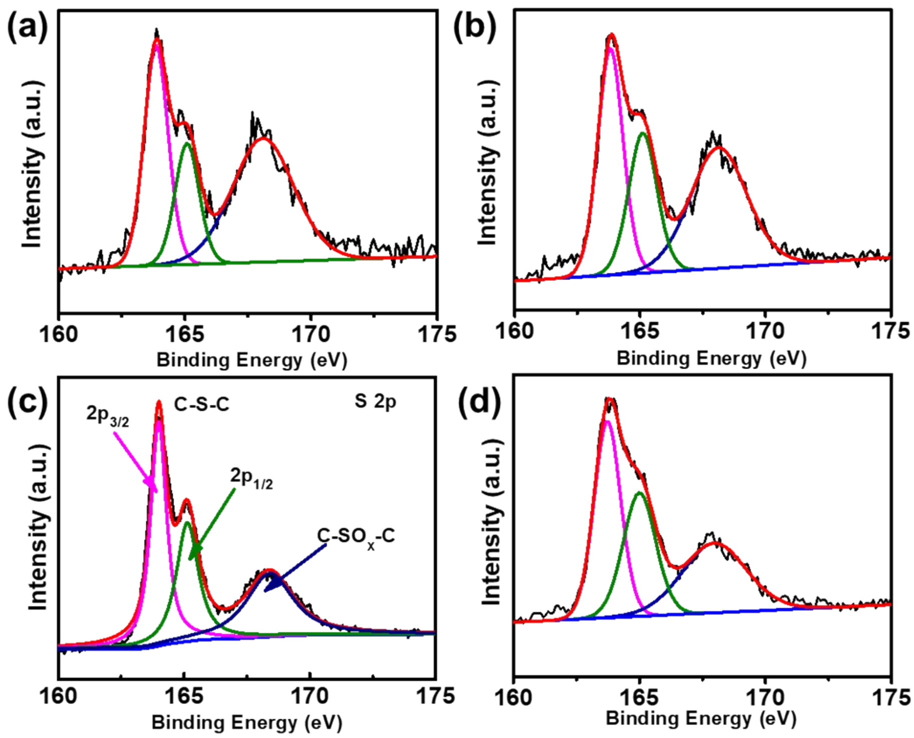

Fig. S14. S2p fitting results of SNC synthetized with different fast pyrolysis temperatures. (a) 800 ℃ (b) 900 ℃ (c) 1000 ℃ (d) 1100 ℃.

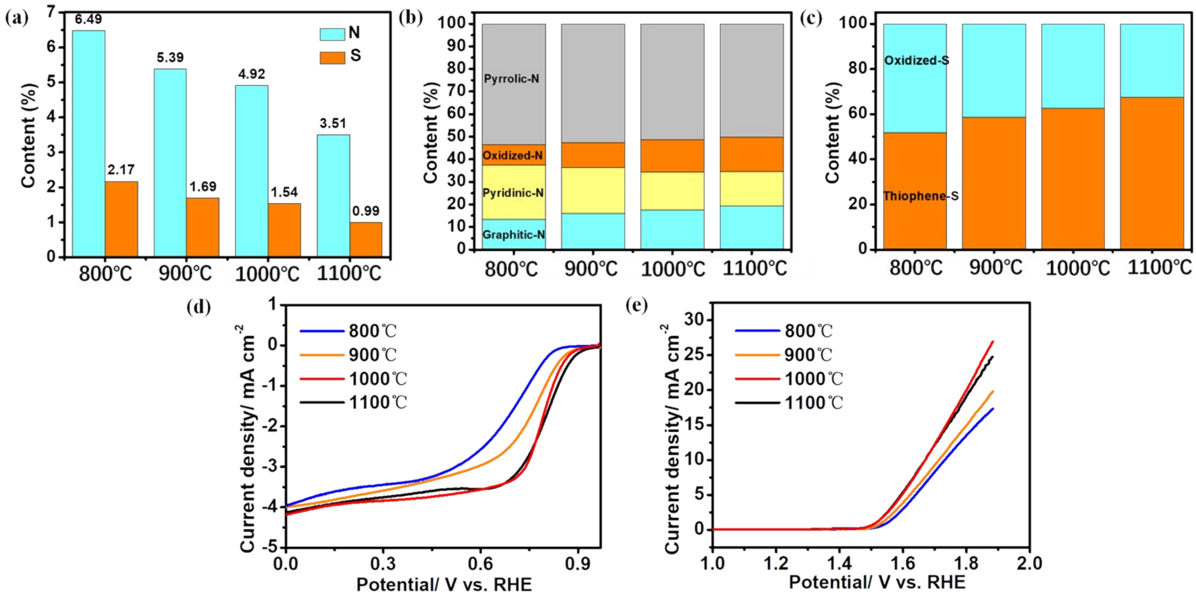

Fig. S15. (a) The total contents of N and S. (b, c) The relative contents of different configurations of N and S. (d, e) ORR and OER LSV curves of SNC synthetized with different fast pyrolysis temperatures.

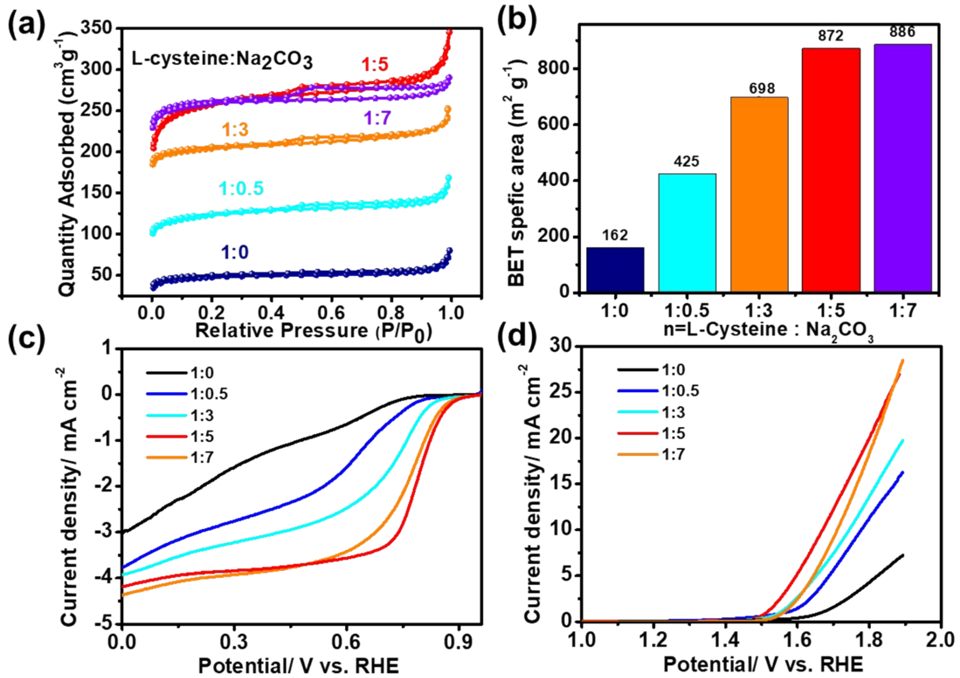

Fig. S16. (a) N_2 adsorption-desorption isotherm curves, (b) BET specific surface area, (c) ORR and (d) OER LSV curves of SNC synthetized with different proportions of L-cysteine and Na_2CO_3.

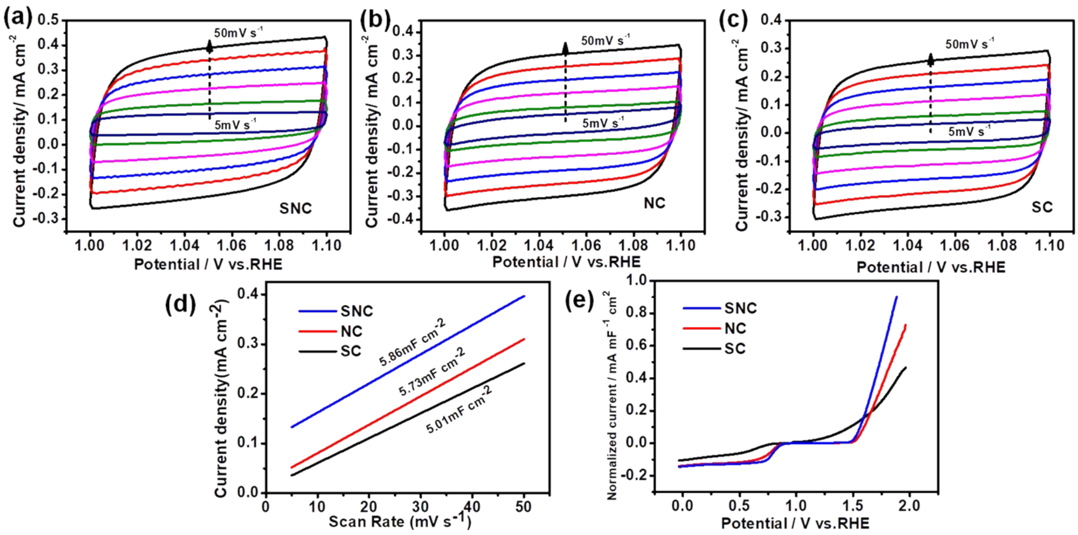

Fig. S17. CV curves at various scan rates within a potential window from 1.0 to 1.1 V vs. RHE without Faradaic processes: (a) SNC, (b) NC, and (c) SC, (d) Charging current densities with different scan rates. The slopes of the straight lines are equivalent to the double-layer capacitance (Cdl). (e) LSV curves of different catalysts for ORR and OER, the current is normalized to electrochemical active surface area.

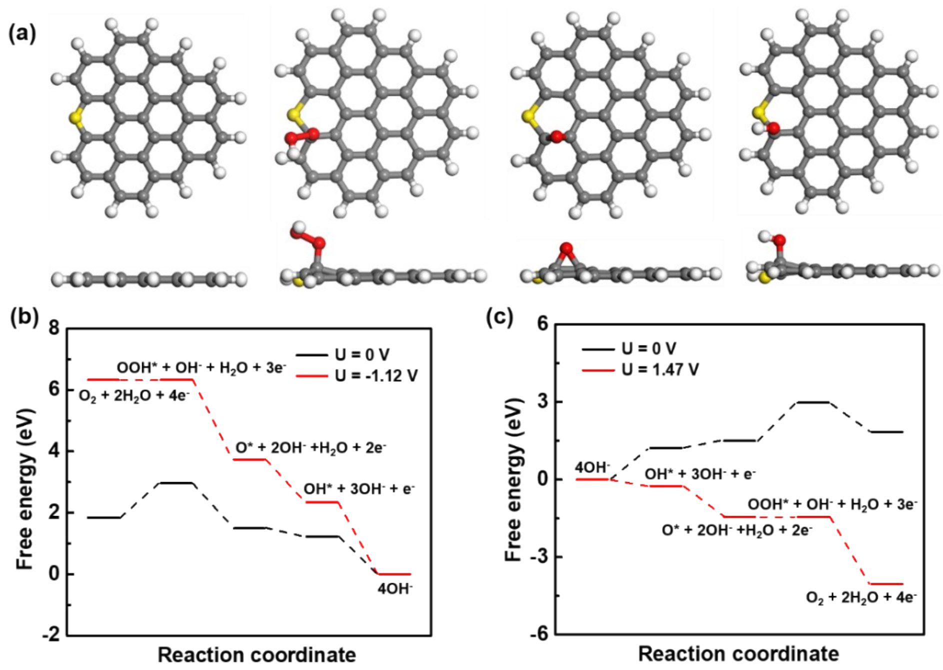

Fig. S18. a) Initial structure and structures after adsorbing OOH*, O*, and OH* intermediates on sulfur-doped graphene. The C, H, O and S atoms are shown in gray, white, red and yellow, respectively; b, c) Free energy diagrams for ORR/OER on the sulfur-doped graphene in alkaline media.

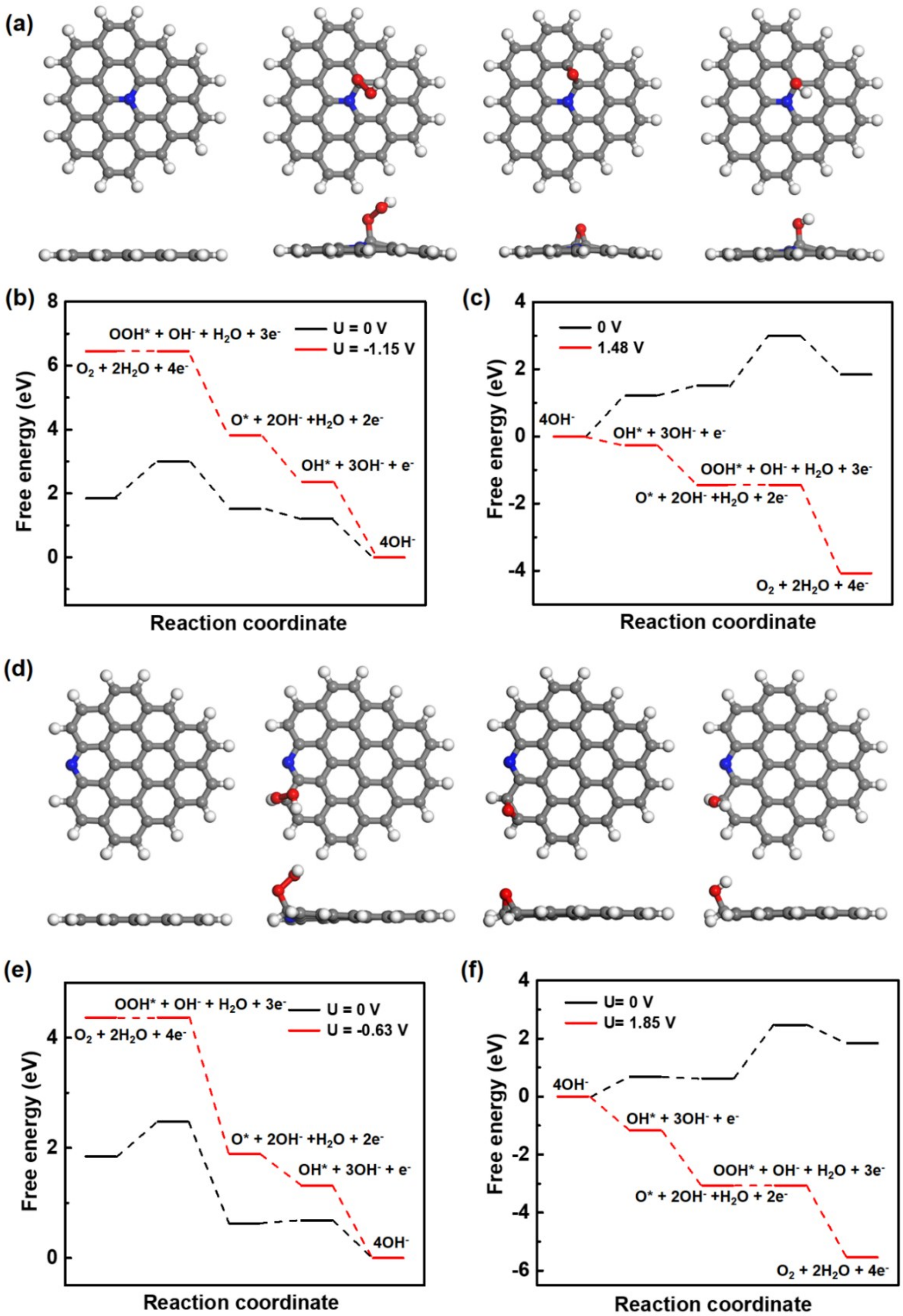

Fig. S19. a, d) Initial structure and structures after adsorbing OOH*, O*, and OH* intermediates on grN-G/pyN-G. The C, N, H and O atoms are shown in gray, blue, white and red, respectively; b, e) Free energy diagrams for ORR on the grN-G/pyN-G in alkaline media; c, f) Free energy diagrams for OER on the grN-G/pyN-G in alkaline media.

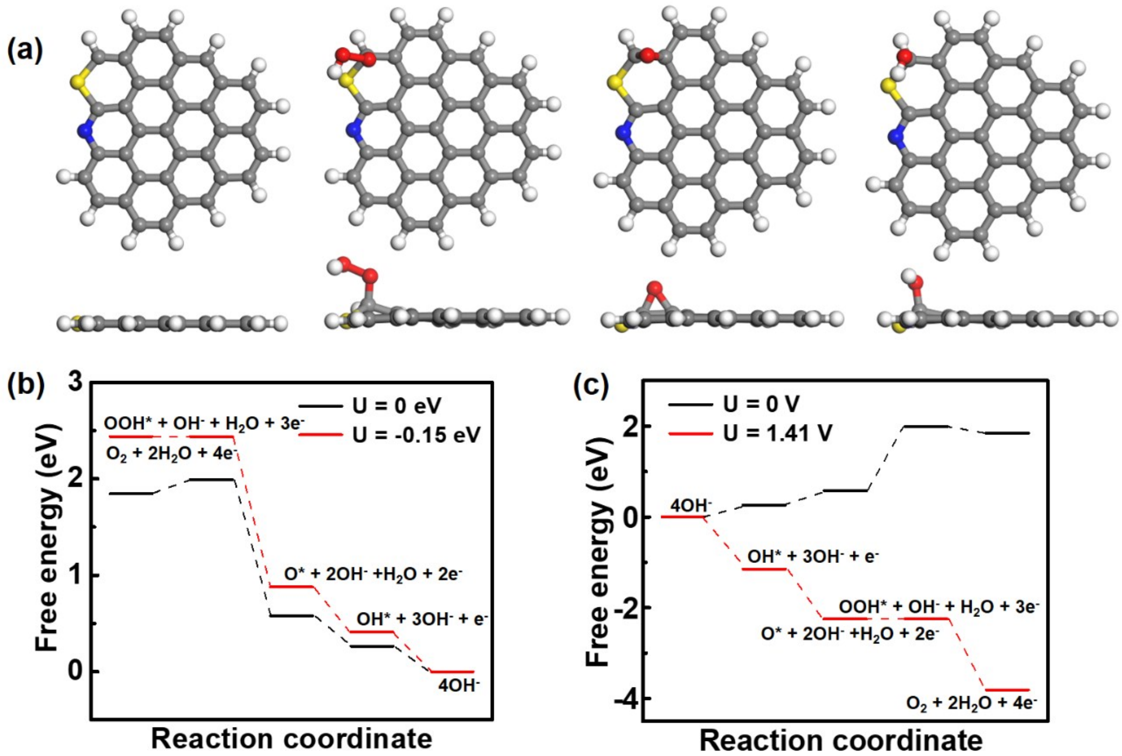

Fig. S20. a) Initial structure and structures after adsorbing OOH*, O*, and OH* intermediates on pyN-S-G. The C, N, H, O and S atoms are shown in gray, blue, white, red and yellow, respectively; b, c) Free energy diagrams for ORR/OER on the pyN-S-G in alkaline media.

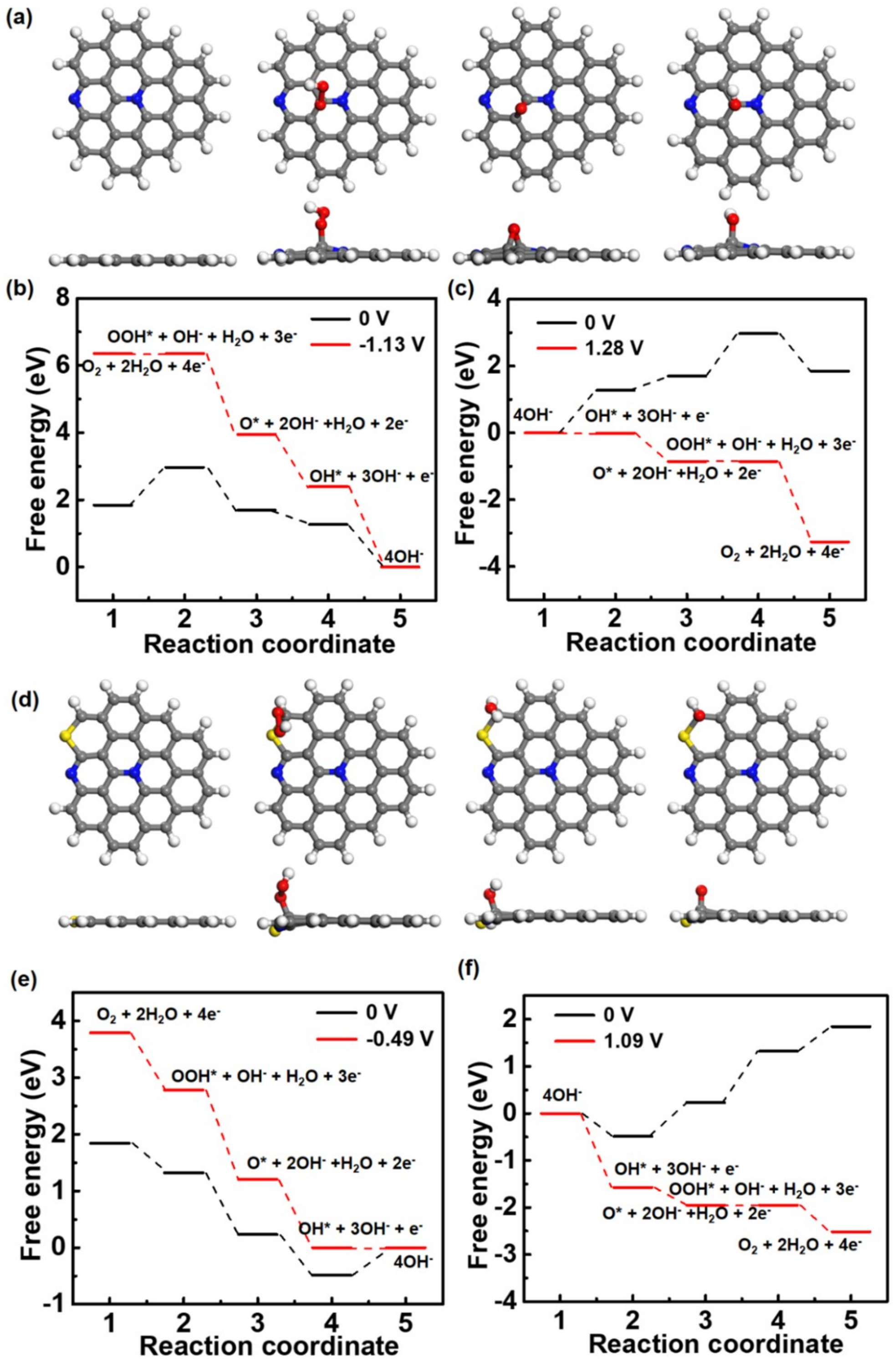

Fig. S21. a, d) Initial structure and structures after adsorbing OOH*, O*, and OH* intermediates on grN-pyN-G/ grN-pyN-S-G. The C, N, H, O and S atoms are shown in gray, blue, white, red and yellow, respectively; b, e) Free energy diagrams for ORR on the grN-pyN-G/ grN-pyN-S-G in alkaline media; c, f) Free energy diagrams for OER on the grN-pyN-G/ grN-pyN-S-G in alkaline media.

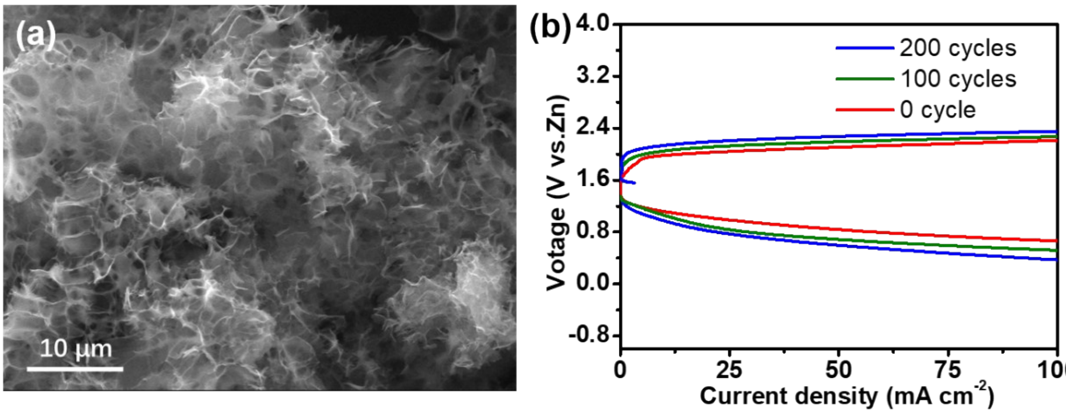

Fig. S22. (a) SEM images of SNC obtained after 200 cycles (1 h per cycle). (b) Charge and discharge polarization curves of batteries after different cycles.

Table S1 Element contents (at. %) and N 1s/S 2p fitting results of SC, NC and SNC.

Catalyst	C	O	N	S	N 1s				S 2p	
					pyridinic	pyrrolic	graphitic	oxidized	thiophene	oxidized
SC	88.72	9.65	-	1.63	-	-		-	50.84	49.16
NC	86.13	8.84	5.03	-	17.31	49.23	19.02	14.44	-	-
SNC	84.81	8.73	4.92	1.54	16.77	51.37	17.61	14.25	62.61	37.39
SNC-0	78.82	10.87	6.84	3.47	19.79	55.76	12.92	11.53	44.52	55.48

Table S2 The electrocatalytic performance parameters (vs RHE) of SC, NC, SNC and Pt/C.

Catalyst	ORR			OER	Overall
	E_{onset} [V]	J_L [mA cm^{-2}]	$E_{1/2}$ [V]	$E_{j=10}$ [mA cm^{-2}]	ΔE [V]
SC	0.85	-2.66	0.56	1.88	1.32
NC	0.90	-4.22	0.68	1.75	1.07
SNC	0.96	-4.25	0.78	1.67	0.89
Pt/C	0.97	-4.83	0.82	1.88	1.06
RuO_2	0.82	-3.91	0.62	1.65	1.03

Table S3 Comparisons of electrocatalytic performance (vs RHE) for SNC with other reported bi-functional ORR/OER catalysts in 0.1 M KOH electrolyte.

Catalyst	$E_{1/2}$ [V]	$E_{j=10}$ [V]	ΔE [V]	Reference
N-doped graphene	0.78	1.69	0.91	Small Methods, 2018, 1800144
B, N co-doped porous carbon	0.79	1.82	1.03	Carbon, 2017, 111, 641-650
N-doped porous carbon fiber	0.82	1.84	1.02	Adv. Mater. 2016, 28, 3000-3006
P-doped C_3N_4 on carbon fiber paper	0.67	1.63	0.96	Angew. Chem. Int. Ed. 2015, 54, 4646-4650
N,S codoped porous carbon	0.88	---	---	J. Mater. Chem. A, 2019, 7, 11223-11233.
N,S codoped porous carbon	0.77	---	---	Electrochimica Acta 2018, 266, 17-26
N,S codoped porous carbon	0.83	---	---	Small 2018, 14, 1800563
MnO@Co-N/C	0.83	1.76	0.93	J. Mater. Chem. A, 2018, 6, 9716–9722
Co2P@CoNPG-900	0.81	1.73	0.92	Electrochim. Acta, 2017, 231, 344-353
ZnCoNC-0.1	0.84	1.75	0.91	Nano Research, 2017, 11, 163-173
SNC	0.78	1.67	0.89	This Work

Table S4 Comparisons of electrocatalytic performance for Zn-air batteries with SNC cathodes with other reported ones.

Catalyst	Peak power density [mW cm^{-2}]	Cycling conditions [mA cm^{-2}]	Stability	Reference
NiO-Al-Co/carbon cloth	36.3	5	20 min/cycle for 1000 cycles (333 h)	Electrochim. Acta, 2018, 290, 21-29
MnO/Co/PGC	172	10	60 min/cycle for 350 cycles (350 h)	Adv. Mater., 2019, 31, 1902339
$MnCo_2O_4$@C	40	10	20 min/cycle for 210 cycles (70 h)	J. Power Sources, 2019, 430, 25-31
Co-Ni-S@NSPC	100	10	20 min/cycle for 180 cycles (60 h)	Carbon, 2019, 146, 476-485
B/N co-doped porous carbon	14.6	20	10 min/cycle for 66 cycles (11 h)	Adv. Mater., 2015， 27， 3789-3796
$Fe_{0.5}Co_{0.5}O_x$/NrGO	86	10	2 h/cycle for 60 cycles (120 h)	Adv. Mater., 2017, 29, 1701410
NPMC-1000	55	2	10 min/cycle for 180 cycles (30 h)	Nat. Nanotech., 2015，10， 444-452
NCNT/$Co_xMn_{1-x}O$	81	7	10 min/cycle for 72 cycles (12 h)	Nano Energy, 2016， 20，315-325
SNC	94.8	5	60 min/cycle for 500 cycles (500 h)	This Work